



Plutonium Particles in Samples Extracted from Hanford Tank Waste TX-118 and SY-102: Interim Report

September 2019

EC Buck
SI Sinkov
ES Ilton
S Scott
DL Blanchard

DD Reilly
TG Lach
BK McNamara
GJ Lumetta

DISCLAIMER

This report was prepared as an account of work sponsored by an agency of the United States Government. Neither the United States Government nor any agency thereof, nor Battelle Memorial Institute, nor any of their employees, **makes any warranty, express or implied, or assumes any legal liability or responsibility for the accuracy, completeness, or usefulness of any information, apparatus, product, or process disclosed, or represents that its use would not infringe privately owned rights.** Reference herein to any specific commercial product, process, or service by trade name, trademark, manufacturer, or otherwise does not necessarily constitute or imply its endorsement, recommendation, or favoring by the United States Government or any agency thereof, or Battelle Memorial Institute. The views and opinions of authors expressed herein do not necessarily state or reflect those of the United States Government or any agency thereof.

PACIFIC NORTHWEST NATIONAL LABORATORY
operated by
BATTELLE
for the
UNITED STATES DEPARTMENT OF ENERGY
under Contract DE-AC05-76RL01830

Printed in the United States of America

Available to DOE and DOE contractors from
the Office of Scientific and Technical
Information,
P.O. Box 62, Oak Ridge, TN 37831-0062
www.osti.gov
ph: (865) 576-8401
fox: (865) 576-5728
email: reports@osti.gov

Available to the public from the National Technical Information Service
5301 Shawnee Rd., Alexandria, VA 22312
ph: (800) 553-NTIS (6847)
or (703) 605-6000
email: info@ntis.gov
Online ordering: <http://www.ntis.gov>

Plutonium Particles in Samples Extracted from Hanford Tank Waste TX-118 and SY-102: Interim Report

Status on Samples Analyzed

September 2019

EC Buck
SI Sinkov
ES Ilton
S Scott
DL Blanchard

DD Reilly
TG Lach
BK McNamara
GJ Lumetta

Prepared for
the U.S. Department of Energy
under Contract DE-AC05-76RL01830

Pacific Northwest National Laboratory
Richland, Washington 99352

Abstract

This is an interim report on the characterization of plutonium (Pu) particles from Hanford wastes. Plutonium-bearing particles were found in Hanford Waste Tank solids, SY-102 and TX-118. Based on Scanning Electron Microscopy (SEM) observations the particles in SY-102 were small, typically < 5 to 10 μm in length, and were crystalline plutonium oxide (PuO_2) with an association of other elements at minor levels, including bismuth, phosphate, and iron. Plutonium particles from SY-102 were extracted from the surface mount using the SEM-Focused Ion Beam (FIB) and prepared for Scanning Transmission Electron Microscopy (STEM). This was the first time that this type of analysis of Hanford tank waste solids had been attempted. The STEM analysis indicated a complex co-precipitation of plutonium oxide with bismuth and phosphate. Diffraction and imaging only partially matched with a plutonium phase. Pockets of phosphate and bismuth reside within the plutonium oxide, suggesting that these phases formed at the same time. The SEM analysis indicated that the plutonium particles from TX-118 were a mixed bismuth-phosphate phase and plutonium oxide. These particles will be examined with SEM-FIB later and then will undergo a more detailed examination in the STEM process.

Executive Summary

This is an interim report on microscopy characterization activities at Pacific Northwest National Laboratory (PNNL) on plutonium (Pu) particles from SY-102 and TX-118 samples. A full report will be forthcoming following the completion of the characterization work.

Nuclear criticality safety concerns arise because a small fraction of plutonium inventory in the Hanford tank waste is in the form of large, dense particles that might be segregated from other waste solids by hydrodynamic conditions during waste handling. Initial characterizations have estimated that about 4% of all plutonium in the tank farms is in the particulate form that presents criticality safety concerns. Further characterization of the plutonium particles and inventories is important to develop the criticality safety evaluations necessary to allow handling and processing of these plutonium-bearing wastes. More information is needed on chemical compositions and densities of the plutonium particles to establish potentials for particle segregation under special hydrodynamic conditions.

Concerns also arise because additional, unidentified plutonium inventory might be in plutonium-bismuth-rich particulate forms. While plutonium-bismuth-rich particulates have been observed in laboratory samples, the exact compositions, conditions of formation, and densities of the particles are unknown. Further characterization of particles will provide insight to the Hanford processing sources and support quantification of the plutonium inventories in support of criticality safety evaluation.

Washington River Protection Solutions (WRPS) shipped waste samples that contained plutonium particulates to PNNL for characterization. PNNL conducted experiments to determine the density of the species and provided the identity of the species so that a qualitative estimate of the density can be found.

Scope

This work involved characterization of the plutonium particles in the waste samples with respect to size, density, and composition. The Pu-Bi-rich particulate forms are of special concern with density and compositions to be characterized to support analysis of their conditions of formation.

A technical report prepared to PNNL standards that provides best-available characterization of the particulate plutonium in the sample materials is the deliverable for the work scope. The technical report will be used as reference basis for criticality safety evaluation supporting the Hanford tank farms operations.

Acknowledgments

The authors thank the Radiochemical Processing Laboratory (RPL) Management and Radiological Control for assisting in developing protocols for the analysis of plutonium-bearing materials within the Radiomaterials Microscopy Suite. We thank the staff at Building 222S for providing the SY-102 and TX-118 samples. We thank Washington River Protection Solutions (WRPS) staff David Losey, Gary Cooke, Jake Reynolds, and Bill Callaway for supporting this project. Pacific Northwest National Laboratory (PNNL) is operated by Battelle for the U.S. Department of Energy under the contract DE-AC05-76RL01830.

Acronyms and Abbreviations

APT	atom probe tomography
BF	bright field
BSE	backscattered electron
CBED	Convergent Beam Electron Diffraction
dpm	disintegrations per minute
EDS	X-ray Energy Dispersive Spectroscopy
EELS	Electron Energy-Loss Spectroscopy
FEG	Field Emission Gun
FFT	Fast Fourier Transform
FIB	Focused Ion Beam
HCA	High Contamination Area
HAADF	high angle annular dark field
keV	kilo-electron volt
μm	micrometer
PNNL	Pacific Northwest National Laboratory
RPL	Radiochemical Processing Laboratory
RPT	Radiological Protection Technician
SEM	Scanning Electron Microscopy
STEM	Scanning Transmission Electron Microscopy
TEM	Transmission Electron Microscopy
wt. %	weight percent
WTP	Waste Treatment Plant
XPS	X-ray Photo-Electron Spectroscopy
XRD	X-ray diffraction

Contents

Abstract	iii
Executive Summary	v
Acknowledgments.....	vii
Acronyms and Abbreviations	ix
1.0 Introduction	1
2.0 Experimental Procedure	2
2.1 Micro-structural Analysis of Samples	3
2.2 SEM Magnification Scale	3
2.3 X-ray Energy Dispersive Spectroscopy	4
2.4 Focused Ion Beam SEM.....	5
2.5 Scanning Transmission Electron Microscopy (STEM).....	5
3.0 Results	7
3.1 Reflectance Spectra of SY-102 and TX-118 Solids.....	7
4.0 SY-102 Characterization	9
4.1 Scanning Electron Microscopy and Analysis of SY-102.....	9
4.2 SEM-FIB Lift Out Preparation of SY-102.....	14
4.3 Scanning Transmission Electron Microscopy of SY-102	16
5.0 TX-118 Characterization	21
5.1 Scanning Electron Microscopy and Analysis of TX-118.....	21
6.0 Discussion and Future Work	24
7.0 References	25

Figures

2.1. SEM sample preparation using a glass funnel and a pointed Q-tip sample collector. Note: all parts shown in this image are cold duplicates of the actual set-up assembled in a hazard control area (HCA) fume hood (dark red solid at the vial bottom is iron(III) hydroxide). Immediately after application all disposable parts should be put into a proper waste container and the funnel extensively decontaminated with water, wiped with wet towels, and placed into a sealed bag to store it until next use.....	2
2.2. SEM images of the magnification standard (MRS-4) showing calibration checked at x200, x1000, x4000, and x10000 (Taken 09-2019).....	4
2.3. Spectrum of a bismuth standard showing peaks identified by the NIST program Desktop Spectrum Analyzer 2 (Kelvin 2018-09-26 revision).....	5
2.4. Atomic resolution image of a plutonium oxide material (A). The measured electron diffraction (B) had d-spacings at 0.310 nm, 0.273 nm, 0.192 nm, 0.160 nm, 0.125 nm. (C) This is in good agreement with literature values for (111) <i>0.3109 nm</i> , (200) <i>0.2692 nm</i> , (220) <i>0.1904 nm</i> , (311) <i>0.1624 nm</i> , (331) <i>0.1235 nm</i>	6
3.1. Pictures of SY-102 (left tube) and TX-118 (right tube) samples. Sample colors shown in the image on the left are more realistic but are slightly out of focus. Image on the right offers a better depth of focusing (an aperture priority mode) but the colors appear darker than they really are. Note presence of very fine and electrostatically active particles adhered to inner side of glass walls around the main mass of the material for the TX-118 sample. No such an effect is observed for the SY-102 sample represented by larger, better defined particles	7
3.2. Reflectance spectra of SY-102 and TX-118 samples. Spectra of partially degraded Pu(IV) oxalate and Pu(IV) tetrafluoride are added for illustrative purposes only to show typical shapes and positions of 5f-transitions for pure plutonium compounds.....	8
4.1. SEM image and EDS analysis of a thorium particle.....	9
4.2. SEM image and EDS analysis of a thorium-bismuth particle and a plutonium-rich phase	10
4.3. Agglomeration of particles in SY-102	10
4.4. Elemental maps of particles	11
4.5. SEM images of a plutonium particle taken under different imaging conditions. (A) high voltage BSE image, (B) Low magnification and low voltage SE image, (C) low magnification image of plutonium particle	12
4.6. Elemental maps of the plutonium particle and surrounding area.....	12
4.7. Small particles of boehmite in the SY-102 waste	13
4.8. Located plutonium particle in SY-102 and the extraction process. Elemental maps identify the location of the particle	14
4.9. Another plutonium particle located in the SY-102 wastes with elemental maps.....	15
4.10. HAADF image (A) of plutonium particle extracted from SY-102, convergent beam electron diffraction (CBED) of the plutonium oxide (B), and elemental maps showing the distribution of major elements.....	16
4.11. Higher magnification images of plutonium particle in STEM-HAADF mode and elemental maps .	17
4.12. Collection of STEM images (A) HAADF image, (B) BF image, Electron energy-loss images of plutonium particle in SY-102 using the (C) oxygen K-edge, and (D) the plutonium O _{4,5} edge.....	18

4.13. Elemental map of plutonium particle at the edge showing a calcium phosphate particle adjacent to the plutonium oxide and an aluminum oxide in the lower right-hand corner of the image.....	18
4.14. High resolution HAADF image of plutonium material in SY-102 (A), FFT of the high-resolution image, and (C) HAADF atomic resolution image of atomic columns in plutonium oxide	19
4.15. Elemental maps at very high magnification showing the presence of phosphorus and bismuth accumulations within the plutonium matrix	20
5.1. Three difference particles found in TX-118 with very similar compositions based on EDS analysis.	21
5.2. SEM image of elongated plutonium-particle and compositional analysis.....	22
5.3. SEM images of plutonium particles in TX-118 (A) a smaller 10 μm particle and (B) a larger 20 μm particle.....	23

Tables

4.1. Semi-quantitative analysis of a selection of particles in SY-102 showing major compositions (element wt%).....	11
4.2. List of d-spacings from SY-102.....	19
5.1. Compositional analysis of selected plutonium particles in TX-118	22

1.0 Introduction

This report is focused on recent progress and proposed future work towards characterizing plutonium-bismuth-phosphorus (Pu-Bi-(±P))-rich particles discovered in the sludge fraction of tanks SY-102 and TX-118. The ongoing mystery concerning the source of the Bi that is closely associated with Pu in these tanks is not addressed. As summarized in Delegard and Jones¹, three species of Pu-rich particles (Pu-O, Pu-Bi, and Pu-Bi-P) were discovered in tanks SY-102 and TX-118 in 2004 and 2012, respectively. A more detailed SEM-EDS (Scanning Electron Microscope-X-ray Energy Dispersive Spectroscopy) study of Pu particles in SY-102 was published in 2016 by Reynolds et al.², who preconcentrated Pu by gravitational settling. The morphology of the Pu-Bi particles is striking, often attaining lengths on the order of tens of microns but only up to about five microns thick. This lath-like morphology can appear to be comprised of smaller laths yielding the so-called “petrified wood” appearance. The Pu-Bi-P particles usually had diameters less than ten microns (larger ones appear to be about 20 microns in diameter) and were described as having a “globular” morphology, indicating to the authors that they are either amorphous or aggregates of smaller particles. A major claim in the paper is that both the Pu-Bi and Pu-Bi-P are oxygen rich. If so, this would have important implications for their propensity to settle and accumulate with strong implications regarding the danger of reaching criticality.

However, as discussed by Reynolds et al.², there were uncertainties in quantifying the amount of oxygen associated with the Pu particles. In this regard, an issue that is not resolvable by conventional SEM-EDS is the possibility that the particles might exist as a dense metallic core coated by a thin oxide layer. With respect to Pu-Bi-P particles, it would also be important to distinguish whether they are aggregates or single amorphous structures, where aggregates would have lower net densities. Again, Reynolds et al.² noted that they did not have the spatial resolution to distinguish between these two possibilities.

The advanced electron microscopy facilities recently established in the Radiochemical Processing Laboratory (RPL) are ideal for tackling these challenging issues. First, the JEOL 300F GrandARM STEM system can routinely reach atomic scale resolution and is ideal for resolving the smallest of particles, thereby potentially settling the issue of whether the Pu-Bi-P particles are aggregates or not. Further, electron diffraction can determine whether the particles are amorphous or crystalline and possibly identify the phase. The Thermo-Fisher Helios 660 Scanning Electron Microscopy-Focused Ion Beam (SEM-FIB) can be used to select individual particles and then section them for further study by Scanning Transmission Electron Microscopy- Electron Energy-Loss Spectroscopy (STEM-EELS) and Scanning Transmission Electron Microscopy-X-ray Energy Dispersive Spectroscopy (STEM-EDS). This will enable us to quantify the composition of a particle from the surface to its core and thus better characterize its density. In the following sections we describe preliminary results and prioritize remaining work.

2.0 Experimental Procedure

The technical or operating procedure (RPL-EMO-1 Rev1) was utilized by this project to conduct the microscopy operations. The two samples from SY-102 and TX-118 were received from Building 222S and partitioned into samples suitable for microscopy analysis. The individual materials were a dried powder that had been previously sieved and separated as reported by Reynolds et al. ²

Due to the high levels of contamination, both glass vial containers of SY-102 and TX-118 materials were handled in a High Contamination Fume Hood area. To deposit these materials on the sticky carbon SEM mount, a modified technique previously used for deposition of plutonium oxide and plutonium tetrafluoride samples was used.

***Caution:** Plutonium-containing materials in a highly dispersible powdery form may be highly mobile and need to be handled with the greatest care possible to prevent dispersion when a small subsample is collected using a sampling tool (in this case a pointed Q-tip) is moved from the container to the upper rim of the funnel.*

Figure 2.1 shows the experimental setup used for SEM sample preparation with pictures taken from two different angles. The vial size was 20 ml, inner diameter of the funnel stem was ~4 mm. A 0.5-inch diameter SEM stub was supported by an inverted mushroom-shaped metal piece. The vial was attached to the funnel with a sticky tape for the photograph. During sample preparation, the vial was held securely, while a pointed Q-tip was used to minimize distance between the vial neck and the funnel opening.

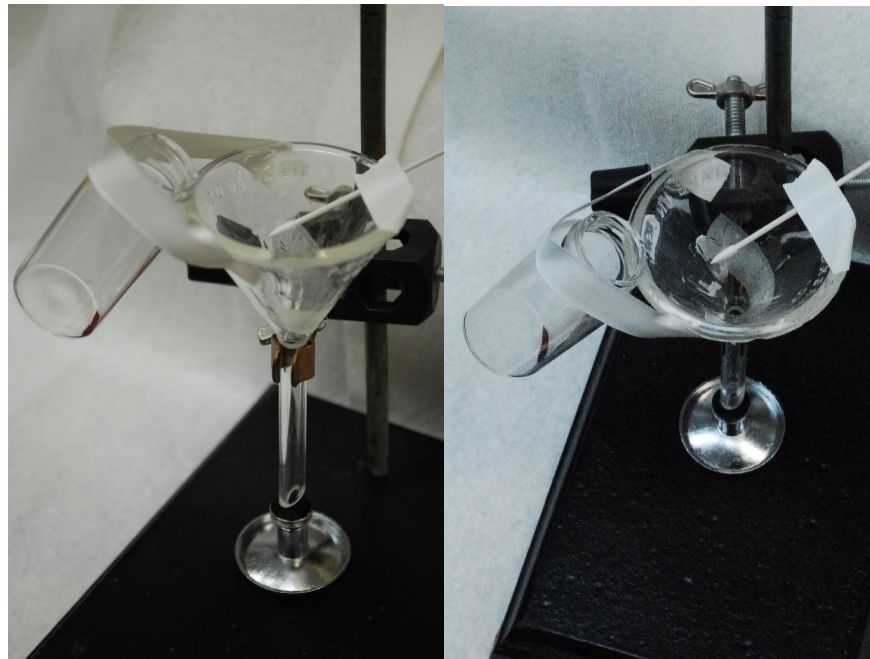


Figure 2.1. SEM sample preparation using a glass funnel and a pointed Q-tip sample collector. Note: all parts shown in this image were cold duplicates of the actual set-up assembled in a High Contamination Area (HCA) fumehood (the dark red solid at the vial bottom is iron(III))

hydroxide). Immediately after application all disposable parts were disposed in a waste container and the funnel was decontaminated with water, wiped with wet towels, and placed into a sealed bag to store.

The use of a bright light source is recommended to illuminate the sticky carbon surface under a very sharp angle after the first round of the material transfer through the funnel to see more clearly the amount of material and its location with respect to the center of the mount. With this light test, if no material was visible on the sticky surface, another round of transfer was performed.

Note: With highly concentrated plutonium powders (PuO_2 , PuF_4 , etc.) a bright light test might not be informative because it only takes a few particles of plutonium to exceed a counting rate of 10^6 disintegrations per minute (dpm) on direct measurement of the sample with alpha meter (this can only be performed by an appropriately trained RPT). This level of alpha activity is considered too risky for application of a tap test and subsequent sample handling unless the requirement is to deposit as many as several hundred particles for a representative size distribution analysis.

Once the material was visibly present, the SEM sample was tap-tested (continuous Radiological Protection Technician (RPT) coverage was required during this process) to confirm that moderate mechanical disturbance of the sample did not lead to release of plutonium particles from the sticky surface to other areas. In the case of a successful tap-test (i.e., no spread of contamination was detected), under RPT instruction, smears were collected from the sides (grooved area) and bottom of the mount. If the smear results were negative the sample could be surveyed out of the HCA. Six samples of SY-102 and two samples of TX-118 were prepared as described above, most of them on an ultra-smooth carbon tape.

2.1 Micro-structural Analysis of Samples

For SEM, a small quantity of the solid material was placed on a flat sticky carbon tape mounted on an aluminum stub using a mini-funnel. This method prevents the spread of particles and reduces the risk of contamination. The sample was then tested for loose particles by gently tapping the specimen on its side. The specimen was then surveyed and checked for smearable activity. The SEM sample was examined in a FEI Quanta250 Field Emission Gun (FEG) equipped with a backscattered electron (BSE) detector and EDAX Genesis X-ray energy dispersive spectrometer (EDS) system in the 325 Building. No conductive carbon coat was used for sample preparation and the instrument was sometimes operated in the low-vacuum mode. This enabled analysis of all major elements in the phases. It is not possible to extract quantitative data or even semi-quantitative data on the light elements, but the analysis can confirm their presence. Examples include the identification of a sodium phase and carbonates.

2.2 SEM Magnification Scale

Most SEM images were obtained at 20 keV with backscattered imaging to enable the high atomic number (Z) phases to be easily viewed. As the sample was not a polished flat section, it is unreliable to extract quantitative data from the EDS analyses; however, semi-quantitative analysis is reported. Analyses

where the lower energy X-rays were present were deleted from consideration. The SEM magnification scale was calibrated with a National Institute for Science and Technology (NIST) traceable standard. The SEM images of this measurement standard are shown in Figure 2.2. The instrument indicated magnification was within one percent of the expected value. The energy scale was checked by looking at high and low energy X-rays from known materials. For SEM, a small quantity of the solid material was placed on a sticky carbon tape mounted on an aluminum SEM stub. The SEM sample was examined in a FEI Quanta250 FEG equipped with a backscattered electron (BSE) detector and EDAX Genesis X-ray EDS system in the RPL.

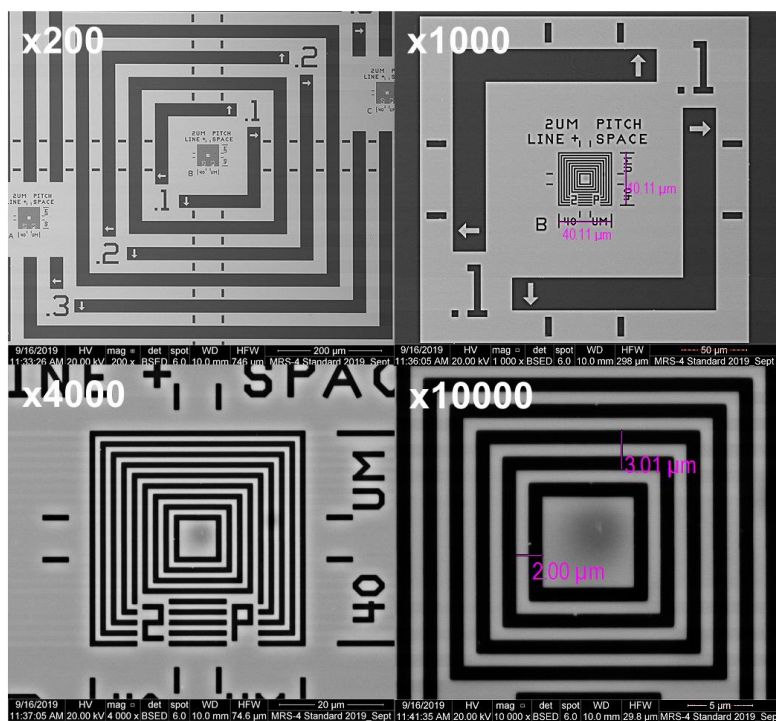


Figure 2.2. SEM images of the magnification standard (MRS-4) showing calibration checked at x200, x1000, x4000, and x10000 (Taken 09-2019)

2.3 X-ray Energy Dispersive Spectroscopy

The EDS system was calibrated with known compounds. The energy positions of peaks measured on the EDS system have been compared to literature values. The agreement between literature and experimental values was excellent, demonstrating that the system is calibrated correctly for analyzing characteristic X-rays at both low and high energies (see Figure 2.3). The error in the peak energy assignments was estimated to be ~1%. Although SY-102 and TX-118 materials were highly radioactive, they did not create any problems for the EDS system.

With the electron beam off, we can record an EDS signal and show the radioactive signature of the material. The TX-118 sample, which was more radioactive than the SY-102 sample, revealed the presence of americium (Am^{241}) through the detection of X-rays from neptunium.

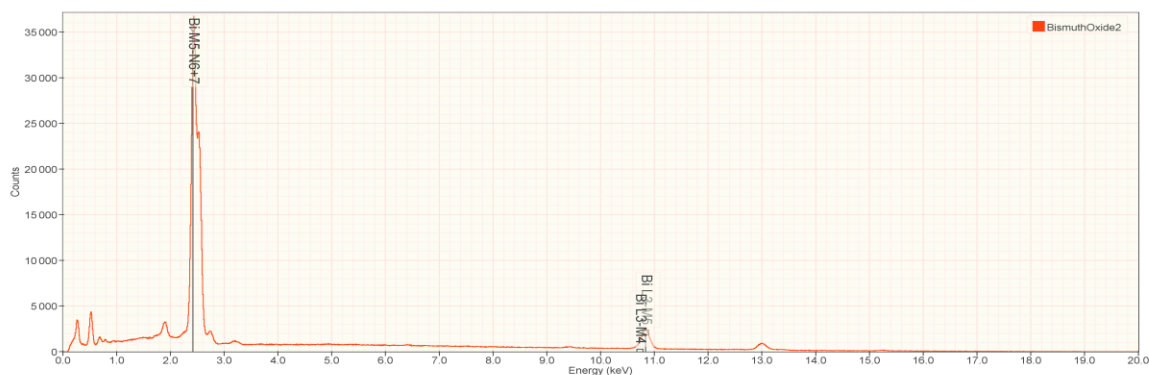


Figure 2.3. Spectrum of a bismuth standard showing peaks identified by the NIST program Desktop Spectrum Analyzer 2 (Kelvin 2018-09-26 revision)

2.4 Focused Ion Beam (FIB) SEM

The SEM mounts containing the dried tank waste specimens were used for locating the Pu particles. A FEI Helios 660 NanoLab™ FEG dual beam focused gallium ion beam/scanning electron microscope (FIB-SEM) equipped with an EDAX (EDAX Inc., Mahwah, NJ) compositional analysis system was used in the Transmission Electron Microscopy (TEM) sample preparation. The current and accelerating voltage of the ion beam used for prep was 9 pA to 9 nA and 2–30 kV, respectively, depending on the progress of the thinning operation. The radioactive contamination state of the chamber was established before and after this process. The thinned specimens were attached to copper (Cu) Omniprobe grids. These were of sufficiently low radioactivity levels that they could be analyzed safely in the GrandARM STEM/TEM.

2.5 Scanning Transmission Electron Microscopy (STEM)

Specimens for Scanning Transmission Electron Microscopy (STEM) were characterized on a JEOL (Japan) ARM300F (GrandARM) probe-corrected microscope equipped with high angle annular dark field (HAADF) and bright field (BF) detectors, dual Bruker X-ray EDS, and Gatan (Gatan Inc., Pleasanton, CA) Quantum Image Filter for Electron Energy-Loss Spectroscopy (EELS). Diffraction patterns, EELS data, and electron micrographs were analyzed with Gatan DigitalMicrograph™ 3.0 software. Resolution and diffraction were demonstrated on a plutonium oxide material shown in Figure 2.4 where the atomic columns were clearly resolved and there was a good match of electron diffraction values to literature values.

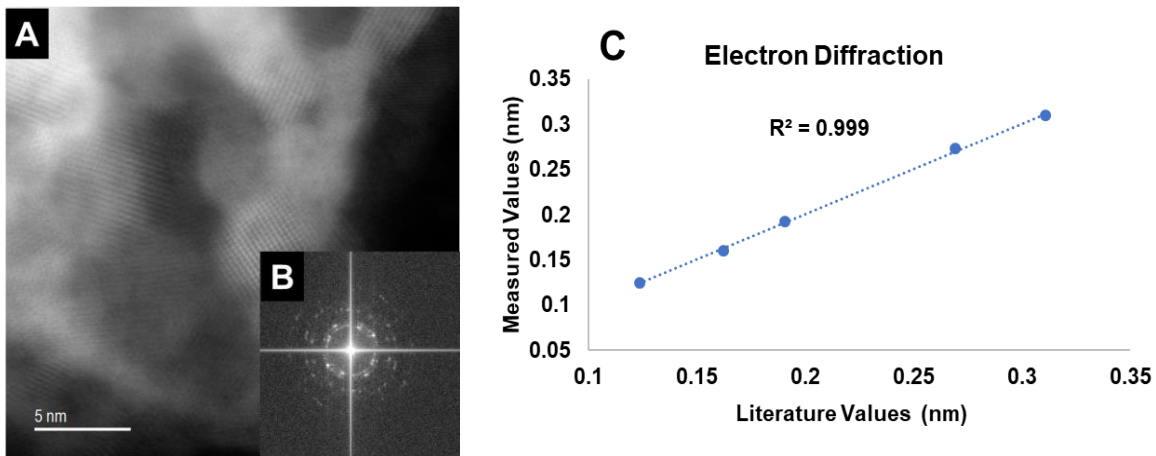


Figure 2.4. Atomic resolution image of a plutonium oxide material (A). The measured electron diffraction (B) had d-spacings at 0.310 nm, 0.273 nm, 0.192 nm, 0.160 nm, 0.125 nm. (C) This is in good agreement with literature values for (111) 0.3109 nm, (200) 0.2692 nm, (220) 0.1904 nm, (311) 0.1624 nm, (331) 0.1235 nm

3.0 Results

This section presents the results of our investigation into the reflectance spectra of the SY-102 and TX-118 sample solids.

3.1 Reflectance Spectra of SY-102 and TX-118 Solids

Small portions (~20 to 25 mg) of the tank solids were placed inside ~10 ml (11.3 mm ID) borosilicate glass round bottom tubes and reflectance spectra were collected in a 380 to 980 nm range of visible spectrum using an Ocean Optics USB2000 spectrophotometer and a high intensity tungsten lamp as a light source. A white powder of aluminum hydroxide loaded into a tube of the same geometry was used as a blank sample. Figure 3.1 shows loaded containers in a horizontal position when the material was broadly spread out along side walls to provide better-quality images. For spectral acquisition the tubes were returned to a vertical position with the solids gently compacted and evenly distributed along the central axis.

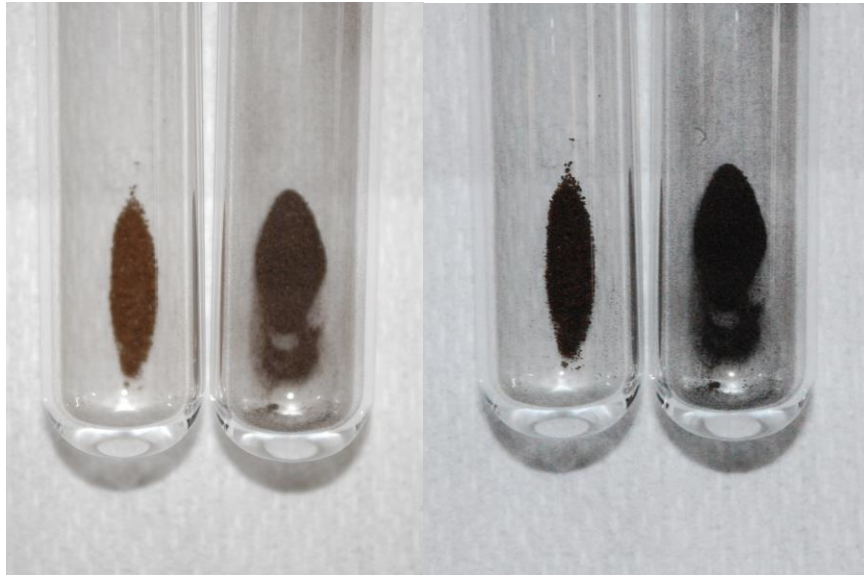


Figure 3.1. Pictures of SY-102 (left tube) and TX-118 (right tube) samples. Sample colors shown in the image on the left were more realistic but were slightly out of focus. Image on the right offers a better depth of focusing (an aperture priority mode) but the colors appeared darker than they really were. Note presence of very fine and electrostatically active particles adhered to inner side of glass walls around the main mass of the material for the TX-118 sample. No such an effect was observed for the SY-102 sample represented by larger, better defined particles

Figure 3.2 shows the reflectance spectra of these samples.

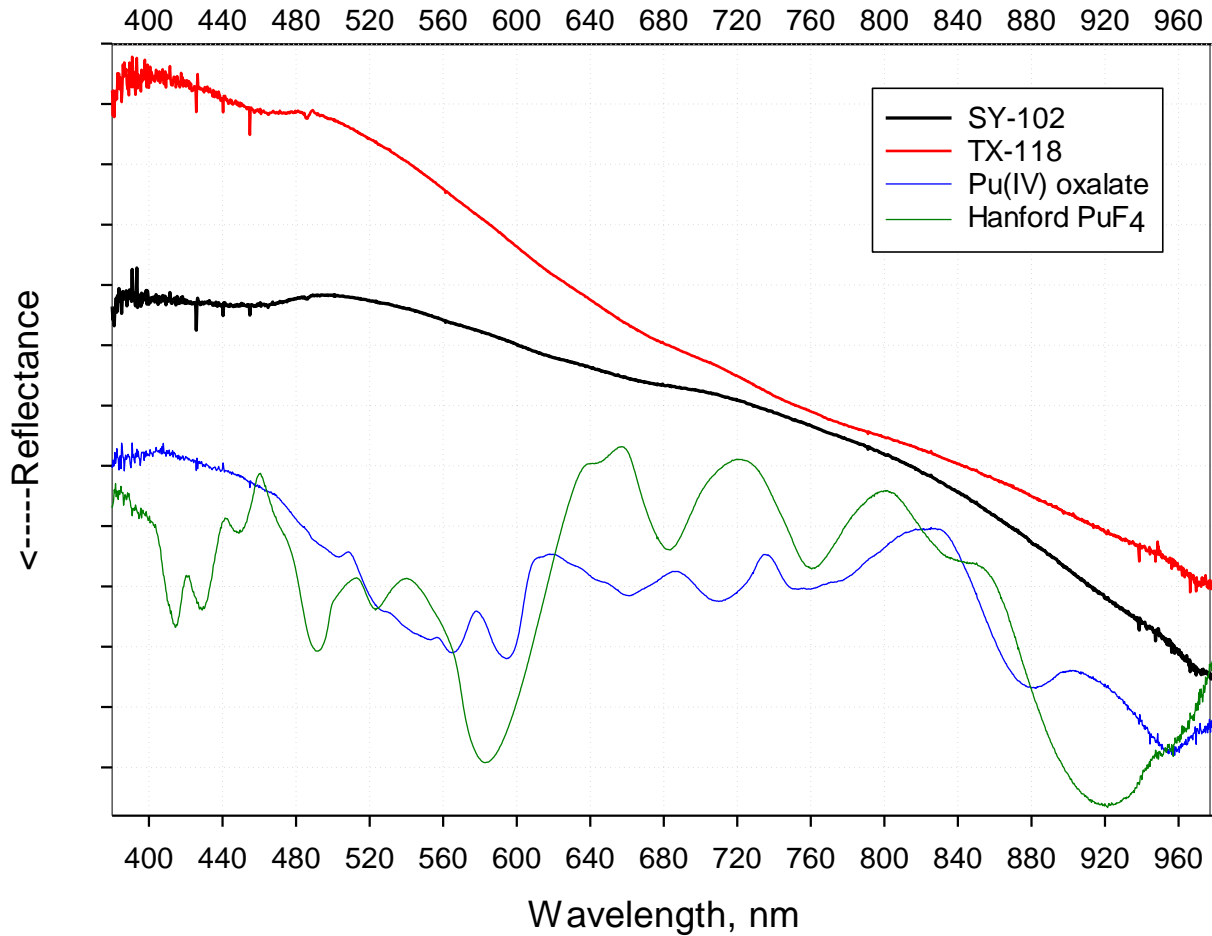


Figure 3.2. Reflectance spectra of SY-102 and TX-118 samples. Spectra of partially degraded Pu(IV) oxalate and Pu(IV) tetrafluoride are added for illustrative purposes only to show typical shapes and positions of 5f-transitions for pure plutonium compounds

As follows from the spectra presented, both samples showed a broad and monotonously changing levels of reflectance signal exhibiting no characteristic peaks across the spectral range examined. This typically happens when plutonium concentration is too low to contribute to any measurable extent to a low reflectance (high absorbance) signal of interfering components represented by iron and other highly colored transition metal compounds in these mixtures. It appears that without additional fractionation to separate the plutonium-rich fraction from bulk of non-radioactive constituents the plutonium signature could not be established reliably in these samples. This was expected based on the total amount of plutonium in the samples.

4.0 SY-102 Characterization

The number of plutonium particles found in SY-102 was low. There were many other particles observed, including particles of thorium-bismuth and uranium. The first step in the analysis work was to examine samples in the SEM to provide an overview of the particles visible in the specimen.

4.1 Scanning Electron Microscopy (SEM) and Analysis of SY-102

The SY-102 material had a range of particle sizes. The BSE detector was used to search for the heavy particles. Many different high Z particles were found but most of these did not contain plutonium. Figure 4.1 and Figure 4.2, contain examples of various particles found in the SY-102 sample. Thorium was commonly found throughout the sample. With BSE imaging in the SEM this phase, together with the uranium and bismuth phases, was difficult to separate from plutonium-bearing particles, so EDS analysis had to be used to distinguish the particles.

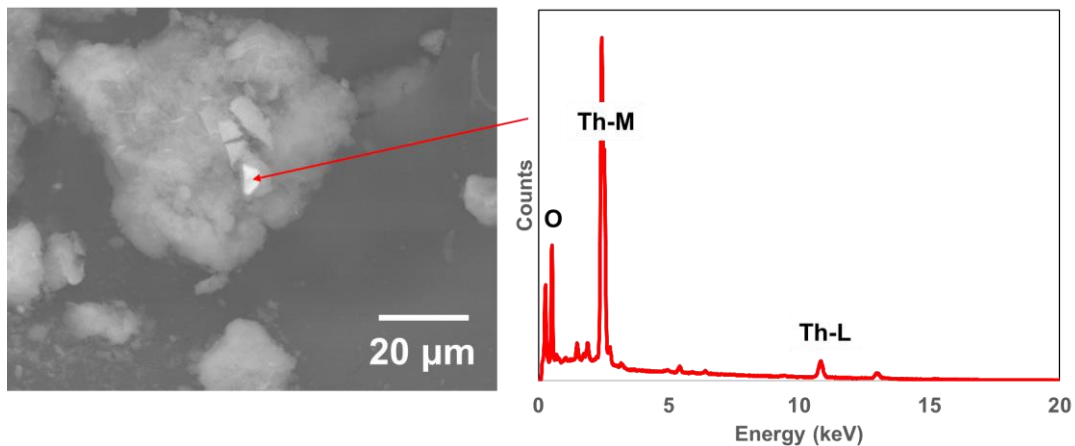


Figure 4.1. SEM image and EDS analysis of a thorium particle

All the high Z particles were extremely small, around 2-5 micrometers in length. The samples themselves had a large variety of particle sizes. In Figure 4.3, a large central particle is shown together with a lot of other material with a diversity of shapes and sizes. Elemental mapping of this region is shown in Figure 4.4 and this shows the composition of the individual particles varied although much of the area appeared to contain bismuth, iron and silicon. There was a particle of chromium, possibly metallic based on the very strong signal obtained. There was also distinct aluminum phases and a calcium-phosphorus phase. There was a small particle in the center of the image that may contain plutonium. The low-level signal of plutonium that appears to suggest uniform coverage was probably an artifact. Unless the particle was identified by both BSE imaging and EDS analysis, the presence of plutonium could not be verified.

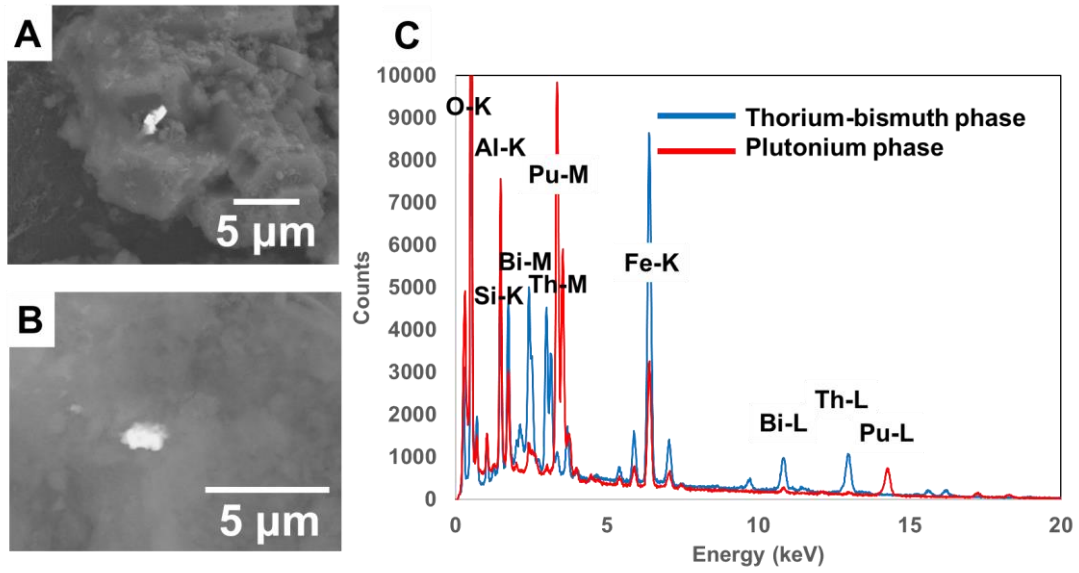


Figure 4.2. SEM image and EDS analysis of a thorium-bismuth particle and a plutonium-rich phase

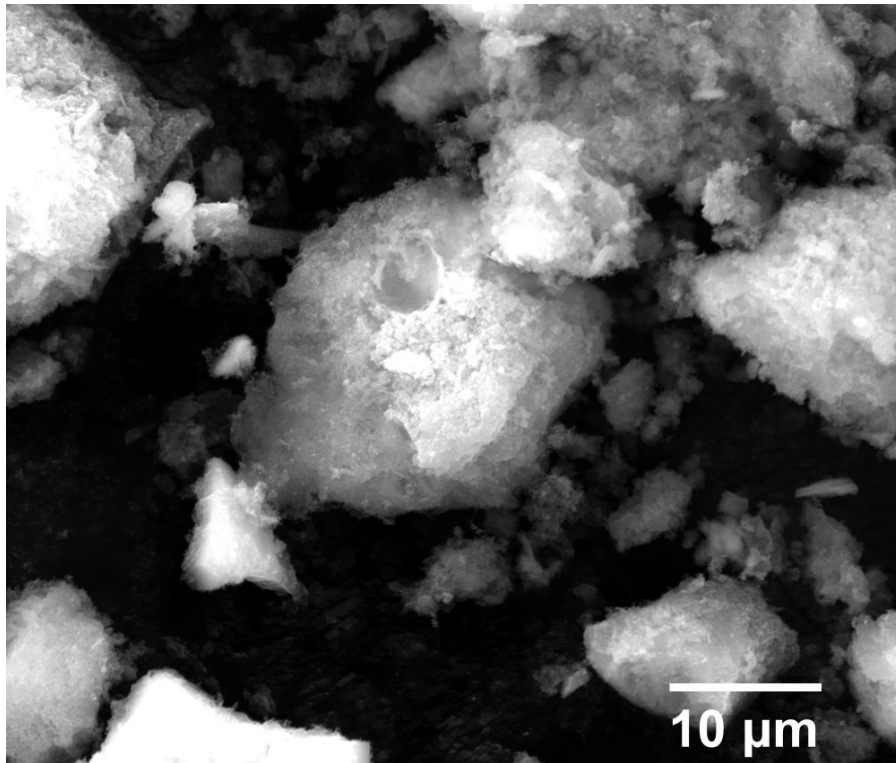


Figure 4.3. Agglomeration of particles in SY-102

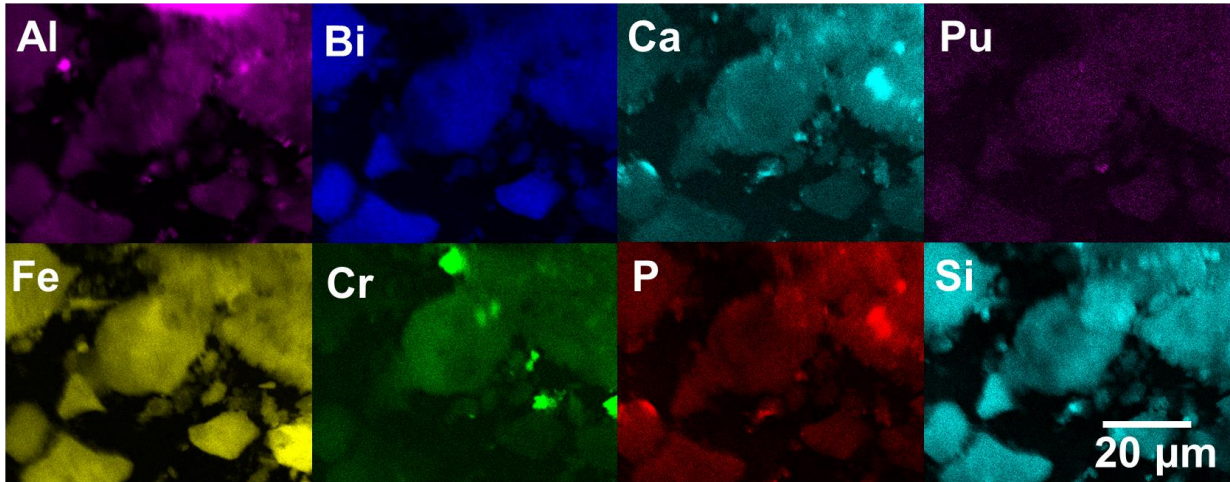


Figure 4.4. Elemental maps of particles

The BSE imaging can be deceptive in describing the morphology of the Hanford tank waste sample. In Figure 4.5, three images are shown in the figure. Under BSE imaging, the plutonium particle is visible but high contrast is also seen for some of the larger particles in the area. As the beam energy was lowered, the surface relief became clearer. The plutonium particle was then shown to be intimately wrapped in the other non-plutonium phases within the sample. The surface had a “wooden-like” look to it which has been observed by others.

Table 4.1. Semi-quantitative analysis of a selection of particles in SY-102 showing major compositions (element wt%)

Point	NaK	MgK	AlK	SiK	PK	SK	BiM	PuM	CaK	BaL	CrK	MnK	FeK
1	3.9	2.9	16.3	13.9	1.2	0.5	12.9	1.1	3.3	0.1	3.0	11.8	29.0
2	4.0	1.7	13.3	10.6	0.5	0.6	16.2	0.8	1.9	0.5	1.6	6.9	30.3
3	4.9	1.1	18.3	12.9	0.5	0.6	16.1	0.8	1.9	0.1	1.5	6.0	34.1
4	5.7	1.2	13.9	9.6	9.6	0.3	10.2	0.1	17.3	0.0	1.6	4.9	32.5
5	4.7	0.2	10.3	9.8	0.1	0.7	19.8	0.0	0.7	0.0	0.2	3.9	36.2
6	7.2	0.4	11.8	16.0	0.2	0.4	18.2	0.0	1.3	0.0	0.8	3.7	50.3

Several particles were analyzed during the characterization and an example set of analyses is shown in Table 4.1. The EDS results do not include oxygen or carbon, which are not easily quantified in the SEM. All the particles indicate high concentrations of bismuth as well as silicon, aluminum, and manganese. These results are consistent with the known composition of this waste.

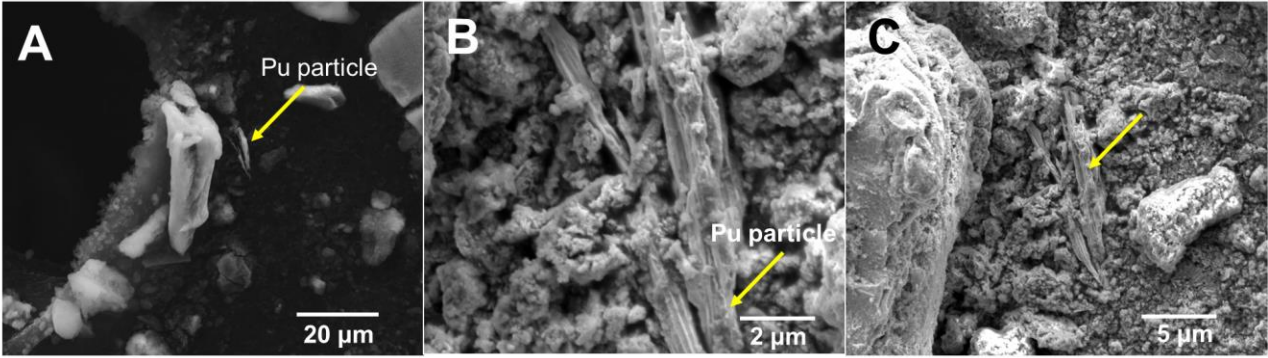


Figure 4.5. SEM images of a plutonium particle taken under different imaging conditions. (A) high voltage BSE image, (B) Low magnification and low voltage SE image, (C) low magnification image of plutonium particle

Elemental analysis of this region is shown in Figure 4.6. Again, much of this material appeared to be a mixed iron-bismuth oxide in agreement with the results in Table 4.1. This type of phase has been described by Lumetta et al.³ in investigations of other Hanford tank waste samples. Because this sample of SY-102 had been density separated, it was reasonable to expect that most of the particles would possess higher densities and for sodium nitrate and aluminum oxide phases to be mainly absent.

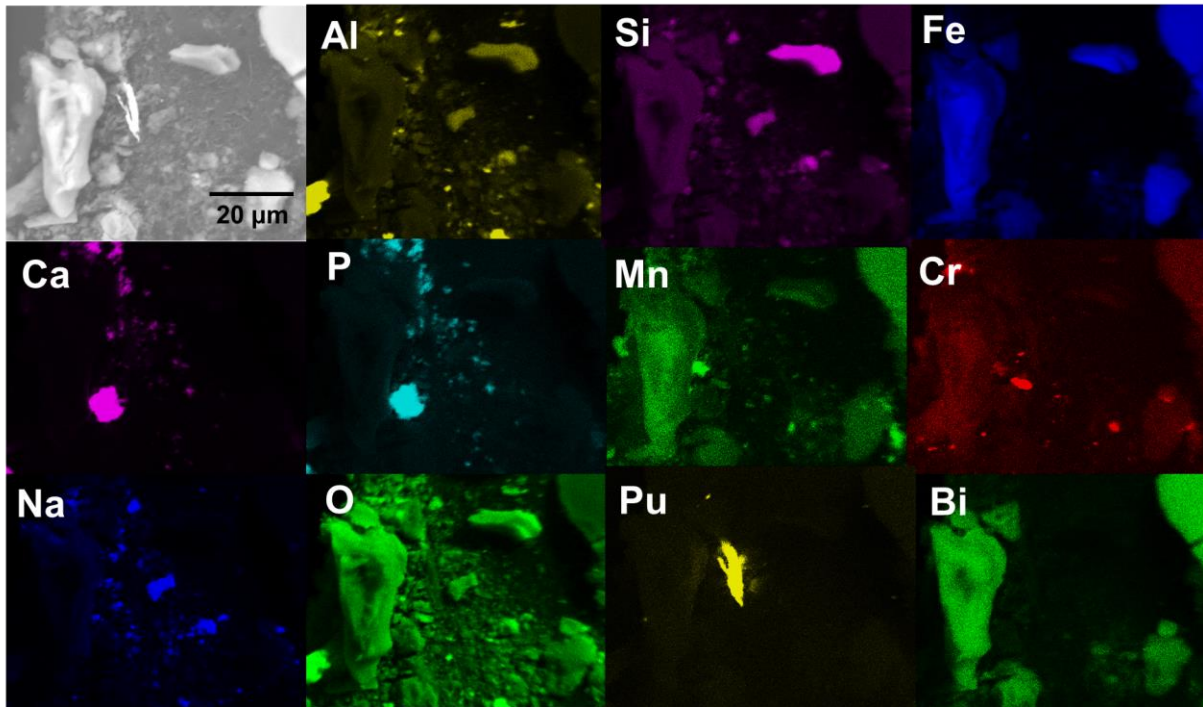


Figure 4.6. Elemental maps of the plutonium particle and surrounding area

Several small boehmite particles were also observed in density separated SY-102 sample. These are very light phases that would not be expected to be present at high concentrations in these samples. Figure 4.7 shows an analysis of the particle using EDS.

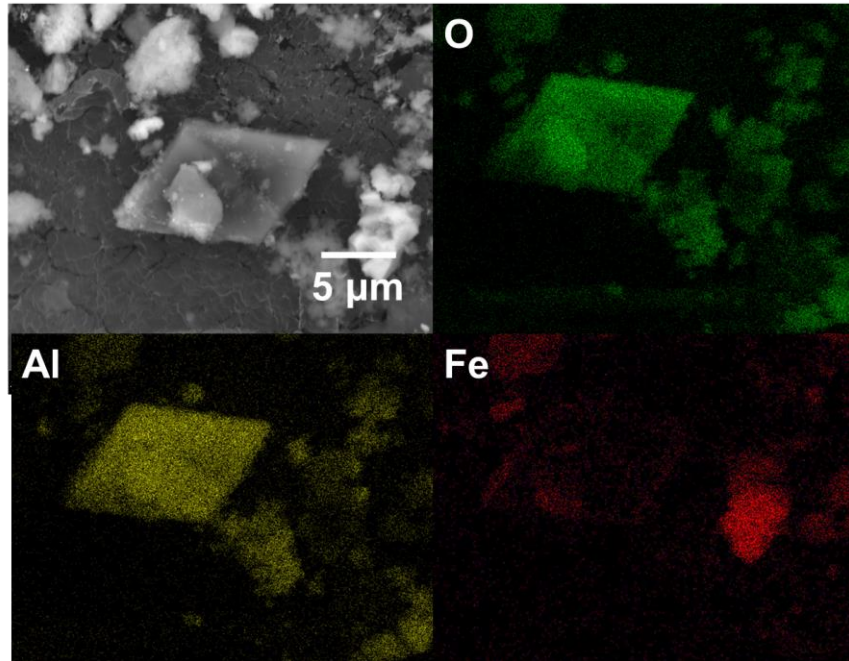


Figure 4.7. Small particles of boehmite in the SY-102 waste

4.2 SEM-FIB Lift Out Preparation of SY-102

Only a few plutonium particles were observed on each SEM stub. When particles were identified they were cut out with the Ga-ion beam. The process of removing a particle from the sample stub first involved coating the sample with carbon to protect the particle from damage from the ion beam. Once the particle was isolated with the ion beam, a probe was brought in and attached to the lift out specimen. This is shown in the images in Figure 4.8.

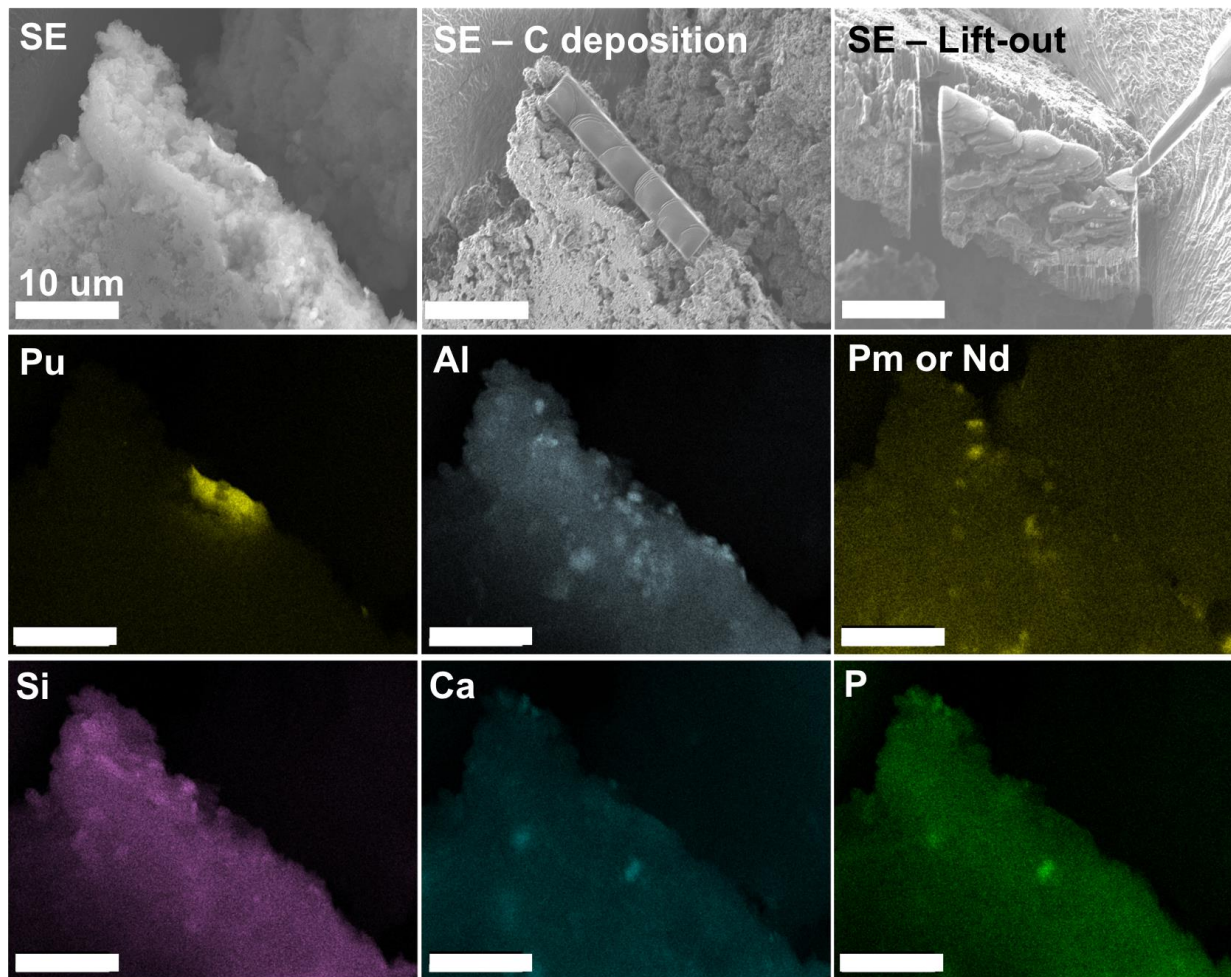


Figure 4.8. Located plutonium particle in SY-102 and the extraction process. Elemental maps identify the location of the particle

Elemental analysis in the SEM-FIB using EDS is also shown in Figure 4.8. Another example of a located particle that was then cut out with the ion beam is shown in Figure 4.9. The plutonium was associated with bismuth and iron as was found in the SEM study.

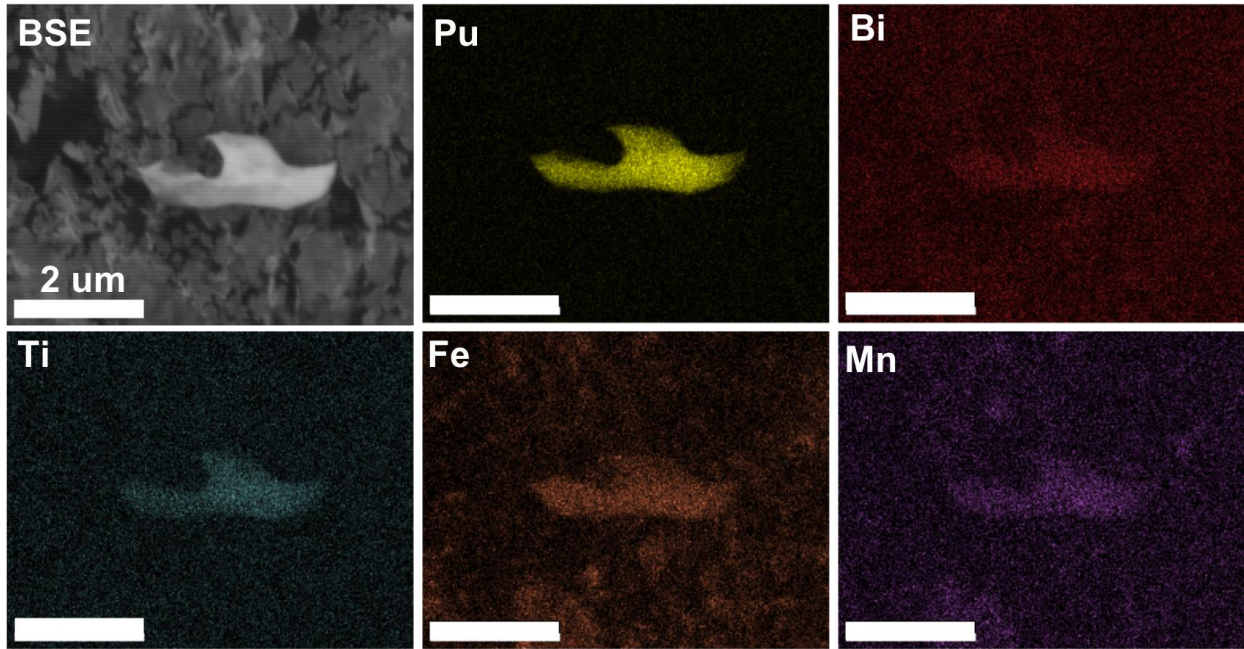


Figure 4.9. Another plutonium particle located in the SY-102 wastes with elemental maps

4.3 Scanning Transmission Electron Microscopy (STEM) of SY-102

STEM was conducted on the lift out specimens produced by the SEM-FIB. The plutonium particle was readily identified during imaging under HAADF imaging. Elemental analysis with EDS was used to establish the major phases in the specimen. In Figure 4.10, the elemental maps are shown. The central particle is plutonium oxide. There is an aluminum oxide particle in the lower right-hand side of the image (A).

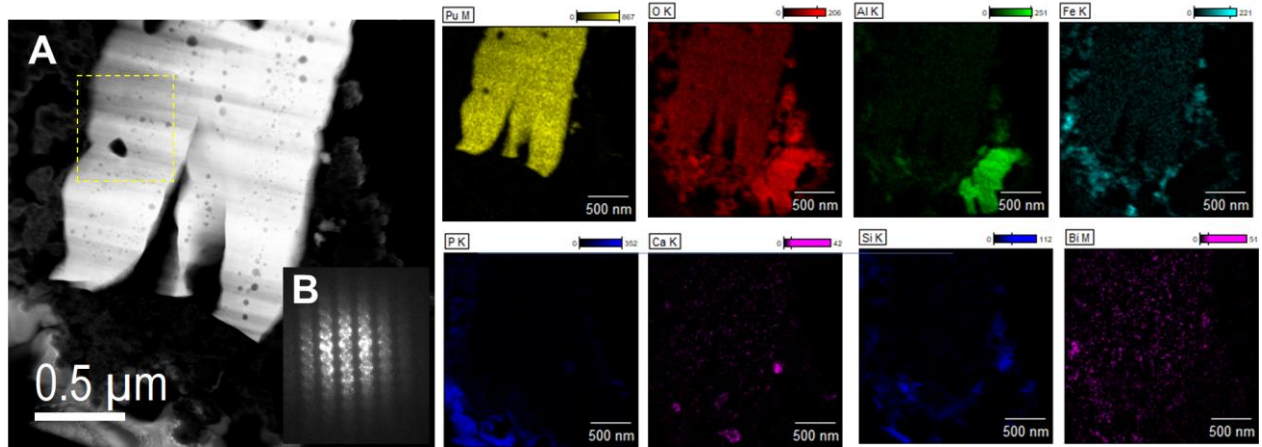


Figure 4.10. HAADF image (A) of plutonium particle extracted from SY-102, convergent beam electron diffraction (CBED) of the plutonium oxide (B), and elemental maps showing the distribution of major elements

Low magnification imaging in the STEM of the plutonium particle from SY-102 strongly suggested that the phase was plutonium oxide (see Figure 4.10). However, other elements were present including aluminum, iron, phosphorus, calcium, silicon, and bismuth. The iron appeared to coat the outer parts of the plutonium but there was some interface between the two phases. Phosphorus and calcium were co-located for the most part and were not directly incorporated into the plutonium phase. Silicon was also heterogeneously distributed. The distribution of bismuth was inconclusive as it appeared to be incorporated into the plutonium material. Slightly higher magnification mapping of this area is shown in Figure 4.11.

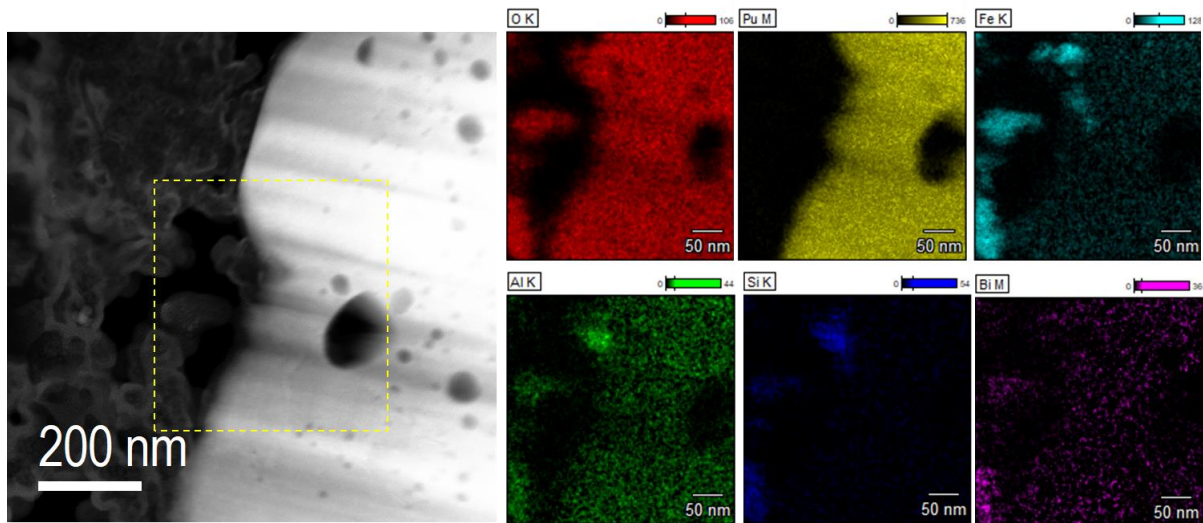


Figure 4.11. Higher magnification images of plutonium particle in STEM-HAADF mode and elemental maps

The major phase is plutonium oxide; however, this phase also has several other elements associated with it including aluminum, iron, and bismuth. The iron appeared to coat the plutonium particles, but the bismuth appeared to be entrained in the plutonium oxide. Higher resolution studies were conducted to determine the exact nature of this association. Another finding from the STEM investigation was that the plutonium particle appeared to have voids or holes in it. This is shown clearly in Figure 4.11. It is possible that the imaging was unable to locate the material in the hole, but the EDS analysis clearly indicates that this is a hole in the structure. The presence of voids in the plutonium phase would severely impact the effective density of the phase.

Analysis of the oxygen level in the phase is not easily accomplished with EDS; however, EELS is a much more effective technique for determining the amount of oxygen in the structure. In Figure 4.12, EELS maps of both plutonium and oxygen can be used to look at the ratio of these two species.

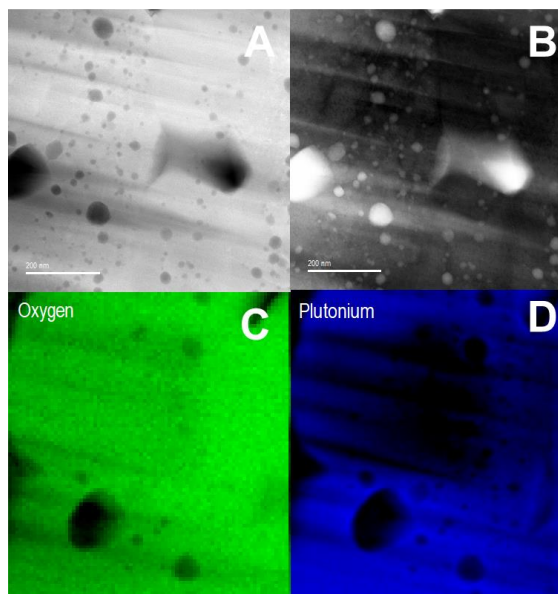


Figure 4.12. Collection of STEM images (A) HAADF image, (B) BF image, Electron energy-loss images of plutonium particle in SY-102 using the (C) oxygen K-edge, and (D) the plutonium $O_{4,5}$ edge

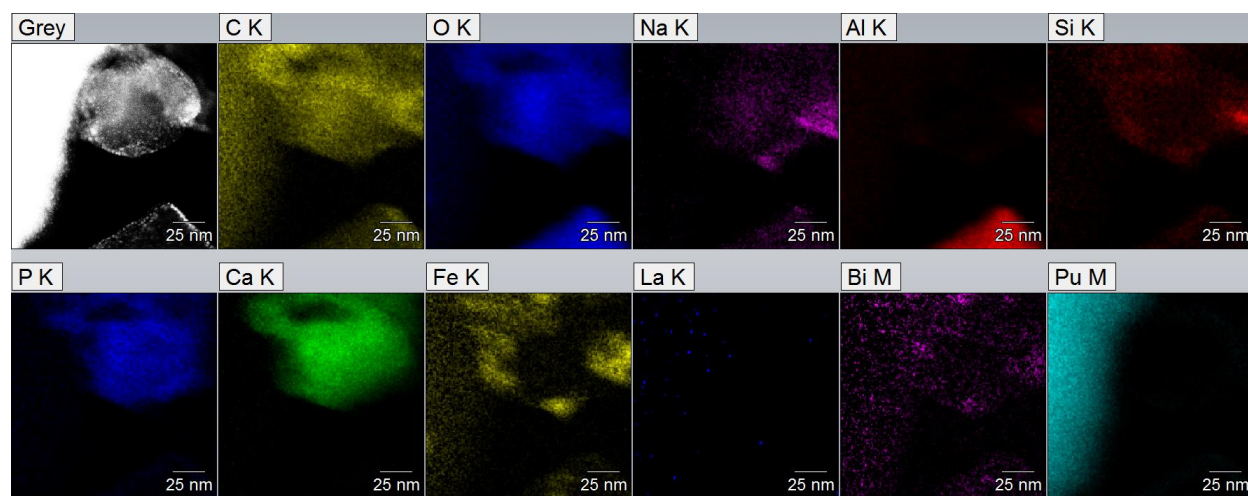


Figure 4.13. Elemental map of plutonium particle at the edge showing a calcium phosphate particle adjacent to the plutonium oxide and an aluminum oxide in the lower right-hand corner of the image

The association of calcium, phosphorus, and oxygen clearly indicates the presence of a calcium phosphate (apatite phase) in the waste specimen. However, this phase is not part of the plutonium phase but merely attached to this particle. An aluminum oxide can also be seen in the image with an association of iron at the edges. The location of bismuth was more difficult to define even at this high magnification. Nevertheless, bismuth seemed to be incorporated into the plutonium oxide phase. The occurrence of spots in the higher magnification HAADF image (see Figure 4.14A) were coincident with the bismuth patches observed in the elemental maps. An atomic resolution image showing atomic columns of the plutonium-bearing structure is shown in Figure 4.14B. Using the Fast Fourier Transform (FFT) of the high-resolution image, it is possible to obtain d-spacings. These are listed in Table 4.2. The values match with plutonium oxide but not exactly. An example of plutonium oxide is shown in the experimental

section (see Figure 2.4). The measured distance between atomic columns in Figure 4.14C were calculated to be 0.195 Å. This is not the Pu-Pu distance in PuO₂ but is close to the Pu-O distance. The Pu-O distance is between 1.8 and 1.9 Å in PuO₂ and PuO_{2+x}. Oxygen atomic columns should not be visible with HAADF imaging.⁴ This suggests that other elements are present in the phase leading to scattering. The arrow in Figure 4.14C points to one of the compositional anomalies or patches that were observed through the plutonium oxide material. The patches and their composition are clearer in the elemental maps in Figure 4.15 that show the enrichment of iron, phosphorus, and bismuth in these regions.

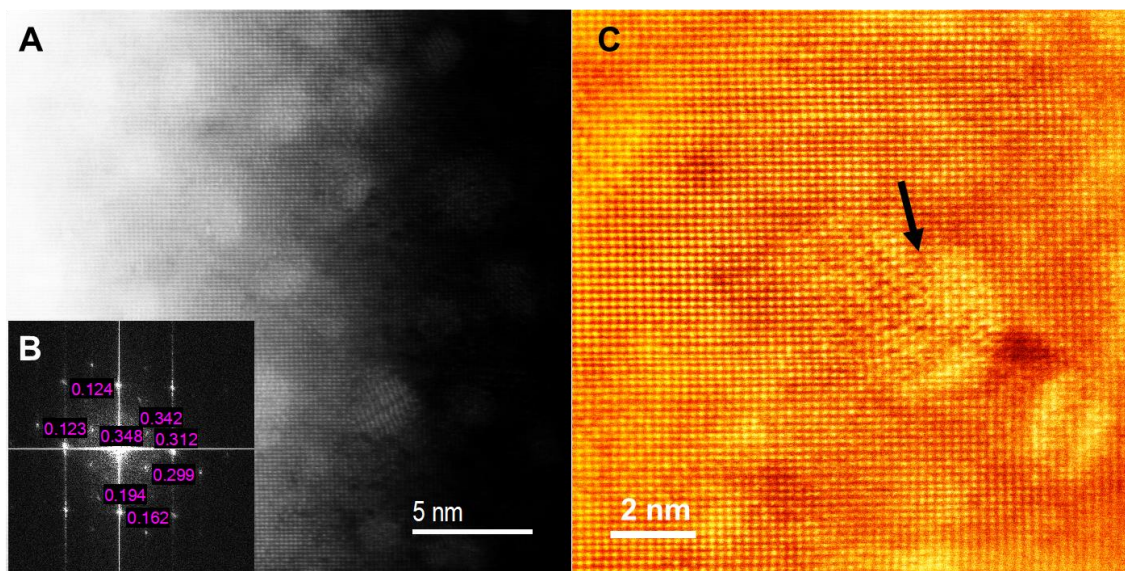


Figure 4.14. High-resolution HAADF image of plutonium material in SY-102 (A), FFT of the high-resolution image, and (C) HAADF atomic resolution image of atomic columns in plutonium oxide

Table 4.2. List of d-spacings from SY-102

Experimental (d-spacings) nm	Literature (PuO ₂) nm
0.348	--
0.342	--
0.312	0.3109
0.299	0.2692
0.194	0.1904
0.162	0.1624
0.124	0.1235

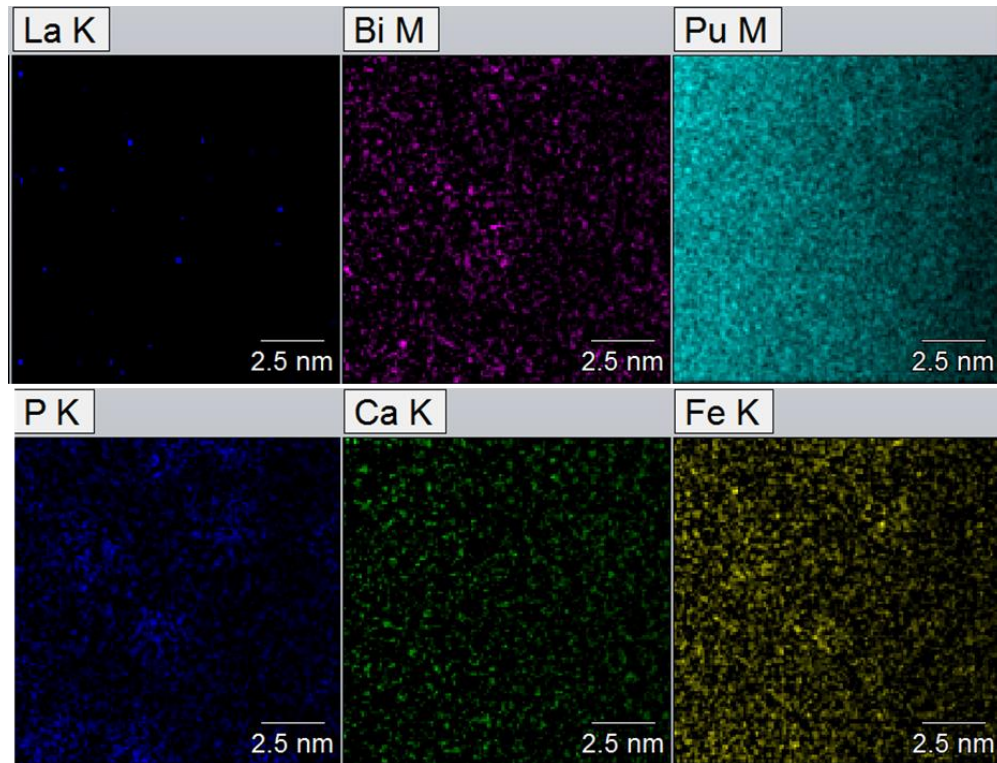


Figure 4.15. Elemental maps at very high magnification showing the presence of phosphorus and bismuth accumulations within the plutonium matrix

The elemental maps show patches of both bismuth and phosphorus within the plutonium oxide, but it is also evident that iron is associated with these phases. This is suggestive of a co-precipitation mechanism and may explain the reason why bismuth, phosphorus, and iron were nearly always found with plutonium in all the analyses. Further work is required to investigate these features and this type of region will benefit from analysis with atom probe tomography (APT) which offers excellent quantification capabilities.

5.0 TX-118 Characterization

This section discusses the SEM investigation and analysis of TX-118.

5.1 Scanning Electron Microscopy (SEM) and Analysis of TX-118

A limited SEM investigation of TX-118 was conducted in this period. The particle size of the TX-118 material was much more homogeneous than the SY-102 sample. Plutonium particles were readily found in this specimen. The particles had a composition that contained bismuth and phosphorus at much higher levels than in the SY-102 sample. In Figure 5.1, the analysis of three particles is shown. In each case, the composition of the particles was extremely consistent.

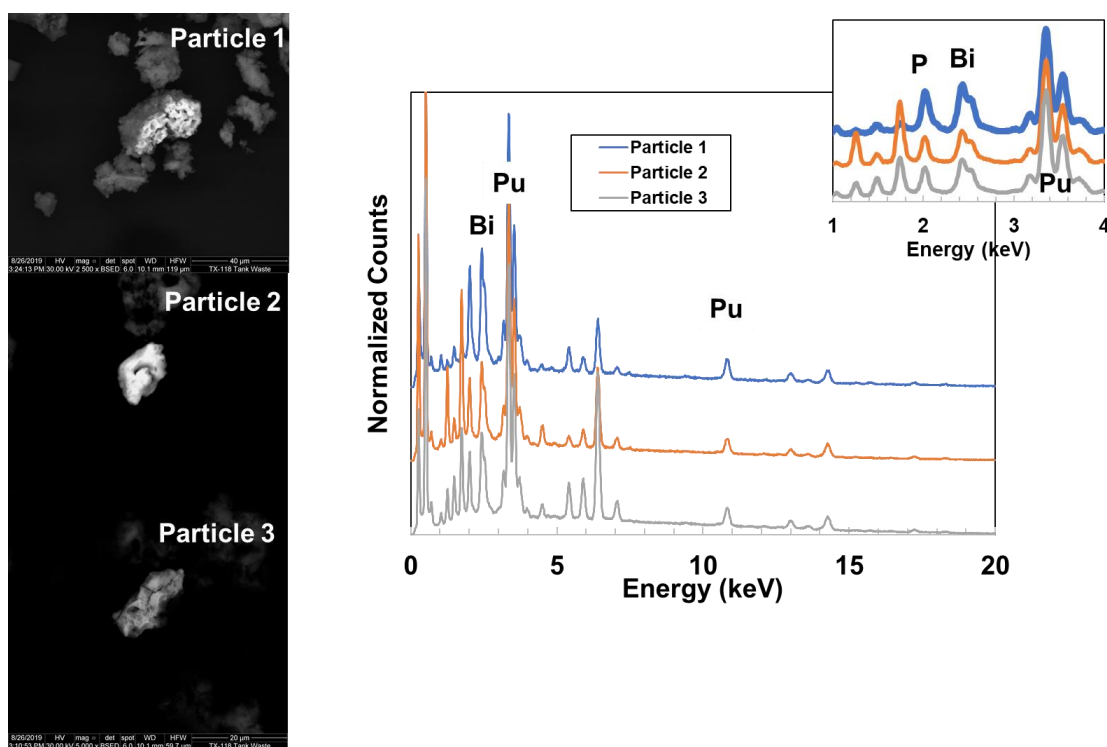


Figure 5.1. Three difference particles found in TX-118 with very similar compositions based on EDS analysis

In Figure 5.2, an elongated particle is shown. This particle was contained within a matrix of aluminum-rich materials. The phase again contained plutonium, bismuth, and phosphorus. Further examples of plutonium particles are shown in Figure 5.3.

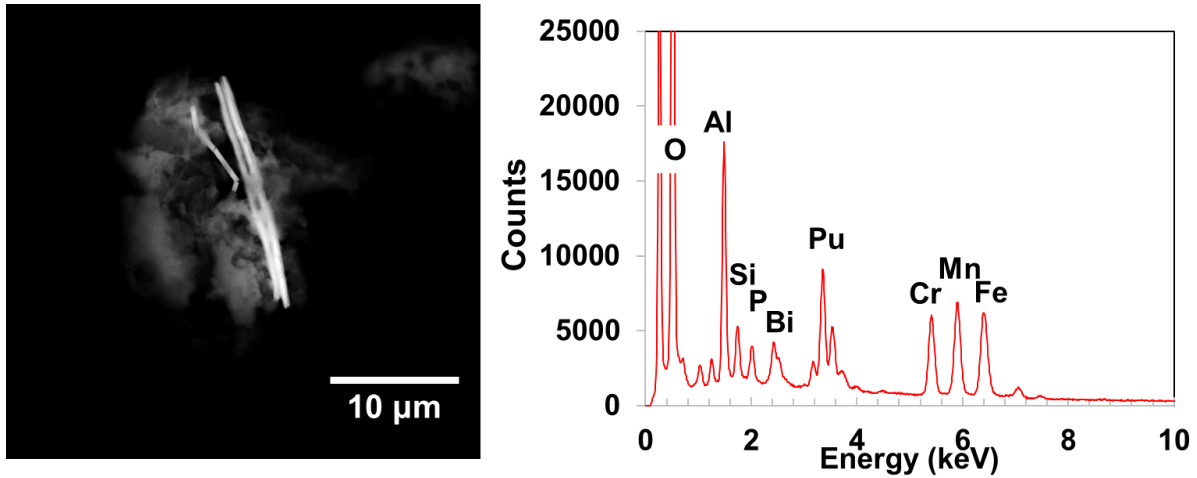


Figure 5.2. SEM image of elongated plutonium particle and compositional analysis

Table 5.1. Compositional analysis of selected plutonium particles in TX-118

<i>Element</i>	<i>Wt%</i>	<i>Wt%</i>	<i>Wt%</i>	<i>Wt%</i>	<i>Wt%</i>
<i>AlK</i>	8.8	3.6	10.1	6.0	1.5
<i>SiK</i>	1.1	3.7	1.6	2.6	1.2
<i>PK</i>	6.2	5.0	5.1	5.1	6.4
<i>SK</i>	0.0	0.0	0.2	0.2	0.4
<i>BiM</i>	15.0	14.1	16.3	14.0	20.6
<i>UM</i>	7.0	6.3	7.5	6.2	7.9
<i>PuM</i>	45.0	48.8	39.9	51.2	50.1
<i>CaK</i>	0.7	0.8	0.7	0.7	0.7
<i>BaL</i>	2.4	0.7	0.0	0.9	0.7
<i>CrK</i>	3.6	2.5	5.4	1.3	2.5
<i>MnK</i>	1.9	2.0	3.7	1.4	1.5
<i>FeK</i>	8.3	12.4	9.6	10.4	6.4
<i>Bi/Pu</i>	0.33	0.29	0.41	0.27	0.41
<i>P/Pu</i>	0.14	0.10	0.13	0.10	0.13

The composition of the particles found in TX-118 was remarkably consistent. In Table 5.1, the compositional analysis (excluding carbon and oxygen) indicate a good correlation between the bismuth, phosphorus, and plutonium concentrations. Further analysis in the STEM will be used to confirm these findings.

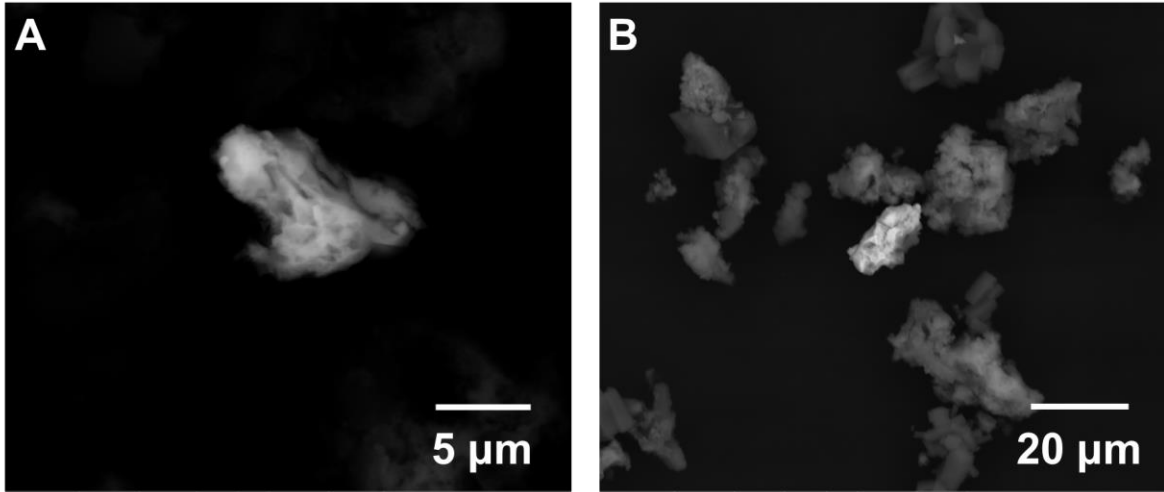


Figure 5.3. SEM images of plutonium particles in TX-118 (A) a smaller 10 μm particle and (B) a larger 20 μm particle

6.0 Discussion and Future Work

The plutonium oxide material in SY-102 was crystalline but contained numerous voids and a significant amount of bismuth and phosphorus. These preliminary results suggest a co-precipitation of the phosphate and bismuth with the plutonium which has resulted in a mixed phase. The overall density of this plutonium phase should be less than pure plutonium oxide because of the element precipitates and the voids. The observation of phosphorus in association with plutonium oxide as nano-precipitates was also found in Z9 crib samples by a team led by Reilly (PNNL) using APT. Use of APT on these samples from SY-102 would help to confirm this result.

Future work will continue to examine more particles from SY-102 and to locate and thin plutonium particles from TX-118. The results are very consistent with the findings of Reynolds et al.; however, it looks more like a co-precipitation mechanism of formation in SY-102 rather than a distinct new phase. Future work will use APT to examine the plutonium particles in SY-102 to better understand the co-precipitation process.

7.0 References

1. Delegard, C. H.; Jones, S. A. *Chemical Disposition of Plutonium in Hanford Site Tank Wastes*; PNNL--23468-Rev.1; Other: 830403000 United States10.2172/1233488Other: 830403000Wed Mar 02 05:21:11 EST 2016PNNLEnglish; 2015; p Medium: ED; Size: 166 p.
2. Reynolds, J. G.; Cooke, G. A.; McCoskey, J. K.; Callaway, W. S., Discovery of plutonium–bismuth and plutonium–bismuth–phosphorus containing phases in a Hanford waste tank. *Journal of Radioanalytical and Nuclear Chemistry* **2016**, *309* (3), 973-981.
3. Lumetta, G. J.; McNamara, B. K.; Buck, E. C.; Fiskum, S. K.; Snow, L. A., Characterization of High Phosphate Radioactive Tank Waste and Simulant Development. *Environmental Science & Technology* **2009**, *43* (20), 7843-7848.
4. Batuk, O. N.; Conradson, S. D.; Aleksandrova, O. N.; Boukhalfa, H.; Burakov, B. E.; Clark, D. L.; Czerwinski, K. R.; Felmy, A. R.; Lezama-Pacheco, J. S.; Kalmykov, S. N.; Moore, D. A.; Myasoedov, B. F.; Reed, D. T.; Reilly, D. D.; Roback, R. C.; Vlasova, I. E.; Webb, S. M.; Wilkerson, M. P., Multiscale Speciation of U and Pu at Chernobyl, Hanford, Los Alamos, McGuire AFB, Mayak, and Rocky Flats. *Environmental Science & Technology* **2015**, *49* (11), 6474-6484.

Distribution

<u>No. of Copies</u>		<u>No. of Copies</u>	
11	PNNL DL Blanchard P7-25 SK Fiskum P7-25 RA Peterson P7-25 GJ Lumetta BK McNamara ES Ilton DD Reilly EC Buck SI Sinkov P7-25		Information Release (PDF) Project File K3-52
		4	Bechtel National, Inc. JG Reynolds H4-02 WS Callaway H4-02 GA Cooke H4-02 D Losey H4-02



**Pacific
Northwest**
NATIONAL LABORATORY

www.pnnl.gov

902 Battelle Boulevard
P.O. Box 999
Richland, WA 99352
1-888-375-PNNL (7665)

U.S. DEPARTMENT OF
ENERGY